J Neurophysiol 113: 3256–3267, 2015.
First published February 18, 2015; doi:10.1152/jn.00714.2014.

Infraslow EEG activity modulates cortical excitability in postanoxic encephalopathy

Michel J. A. M. van Putten,[1,2] Marleen C. Tjepkema-Cloostermans,[1,2] and Jeannette Hofmeijer[2,3]
[1]*Department of Neurology and Clinical Neurophysiology, Medisch Spectrum Twente, Enschede, the Netherlands;* [2]*Clinical Neurophysiology, MIRA-Institute for Biomedical Technology and Technical Medicine, University of Twente, Enschede, the Netherlands; and* [3]*Department of Neurology, Rijnstate Ziekenhuis, Arnhem, the Netherlands*

Submitted 22 September 2014; accepted in final form 17 February 2015

van Putten MJAM, Tjepkema-Cloostermans MC, Hofmeijer J. Infraslow EEG activity modulates cortical excitability in postanoxic encephalopathy. *J Neurophysiol* 113: 3256–3267, 2015. First published February 18, 2015; doi:10.1152/jn.00714.2014.—Infraslow activity represents an important component of physiological and pathological brain function. We study infraslow activity (<0.1 Hz) in 41 patients with postanoxic coma after cardiac arrest, including the relationship between infraslow activity and EEG power in the 3–30 Hz range, using continuous full-band scalp EEG. In all patients, infraslow activity (0.015–0.06 Hz) was present, irrespective of neurological outcome or EEG activity in the conventional frequency bands. In two patients, low-amplitude (10–30 μV) infraslow activity was present while the EEG showed no rhythmic activity above 0.5 Hz. In 13/15 patients with a good outcome and 20/26 patients with a poor one, EEG power in the 3–30 Hz frequency range was correlated with the phase of infraslow activity, quantified by the modulation index. In 9/14 patients with burst-suppression with identical bursts, bursts appeared in clusters, phase-locked to the infraslow oscillations. This is substantiated by a simulation of burst-suppression in a minimal computational model. Infraslow activity is preserved in postanoxic encephalopathy and modulates cortical excitability. The strongest modulation is observed in patients with severe postanoxic encephalopathy and burst-suppression with identical bursts.

infraslow fluctuations; EEG; postanoxic coma; burst-suppression

CLINICAL EEG TYPICALLY RECORDS signals in the 0.1–70 Hz frequency range. However, brain rhythms include activity below 0.1 Hz and far above 70 Hz (Helps et al. 2008; Vanhatalo et al. 2005; Zelmann et al. 2014).

Voltage fluctuations below 0.1 Hz are known as infraslow activity and can be recorded with full-band EEG equipment or systems with a lower frequency limit of at least 0.1 Hz (Rodin et al. 2014). Infraslow activity may have a (nearly) periodic character, resulting in infraslow oscillations. Infraslow activity may be viewed as part of the natural spectrum of rhythmic changes in excitability of neuronal networks and represents an important component of physiological and pathological brain function (Hughes et al. 2011; Ko et al. 2011; Lörincz et al. 2009; Rodin et al. 2014; Schroeder and Lakatos, 2009; Vanhatalo et al. 2004).

Infraslow activity of the neocortex was first reported by Aladjalova in 1957 in rabbits. She recorded rhythms with frequencies of 0.01–0.1 Hz (Aladjalova 1957). The notion of infraslow activity as a modulator of cortical excitability was stressed by her observation of faster oscillations phase-locked to the positive phases of the 0.1 Hz rhythms (Aladjalova 1957). More recently, in humans, the amplitude of EEG at 1–100 Hz was shown to correlate with the instantaneous voltage in the frequency range 0.02–0.2 Hz, and during sleep K-complexes and interictal epileptiform discharges occurred more often at particular phases of the infraslow activity (Vanhatalo et al. 2004). Also, task performance correlated with infraslow EEG fluctuations: stimulus detection probability was 55% larger in the rising than the falling phase of an infraslow fluctuation cycle (Monto et al. 2008). In a study in patients under moderate and deep anesthesia, during nonpulsatile cardiopulmonary bypass surgery, infraslow activity of ~0.06 Hz was observed as well. This was correlated with changes in total EEG power and accompanied by oscillations of the middle cerebral blood flow velocity with similar frequency (Zanatta et al. 2013).

There is a close frequency correspondence between infraslow electrical activity and the changes in resting-state BOLD signal, including the default-mode network (Raichle et al. 2001), where oscillations in the resting-state blood oxygenation level-dependent signal (BOLD) signal with frequencies below 0.1 Hz are a consistent finding (Fox and Raichle 2007; Ko et al. 2011; Rosazza and Minati 2011). This suggests a close linkage, which is indeed supported by various studies. For instance, infraslow components of the local field potentials, as recorded in rat, exhibit correlation with the spontaneous BOLD signal at the recording site (Pan et al. 2013). Spontaneous BOLD signals and slow cortical potentials in humans were also correlated using electrocorticography (He et al. 2008).

In another study involving human subjects, combined EEG/functional MRI (fMRI) during sleep showed correlations between power in the infraslow EEG band and the BOLD signal (Picchioni et al. 2012). Infraslow scalp EEG fluctuations were also correlated with resting state network dynamics using fMRI under task-free conditions (Hiltunen et al. 2014). In this latter study, it was found that independent components of spontaneous infraslow EEG fluctuations were selectively correlated with fMRI-BOLD signals in specific resting-state networks. This recent literature strongly supports the notion that infraslow EEG activity is directly associated with endogenous fluctuations in neuronal activity levels, recorded with fMRI. As the BOLD signal reflects changes in metabolic demand and infraslow activity presumably modulates neuronal activity, which is also accompanied with changes in energy consumption, both appear to reflect a common phenomenon: slow

Address for reprint requests and other correspondence: M. J. A. M. van Putten, Dept. of Neurology and Clinical Neurophysiology, Medisch Spectrum Twente and Clinical Neurophysiology, MIRA-Institute for Biomedical Technology and Technical Medicine, Univ. of Twente, Enschede, the Netherlands (e-mail: m.j.a.m.vanputten@utwente.nl).

modulations of cortical neuronal activity that waxes and wanes across widespread spatial scales.

The mechanisms that cause low-frequency fluctuations remain poorly understood. Aladjalova (Aladjalova 1964) has shown that cortical slabs without any subcortical input can generate infraslow activity. More recently, involvement of subcortical structures, in particular the thalamus, has been proposed (Hughes et al. 2011; Lörincz et al. 2009). For example, oscillations at 0.005 to 0.25 Hz were measured in nuclei of the dorsal thalamus in rats (Albrecht and Gabriel 1994; Albrecht et al. 1998) and in anesthetized guinea pigs in vivo (He 2003). Also, oscillations at 0.005–0.1 Hz were recorded in individual thalamocortical neurons in slices of cat sensory thalamic nuclei. Here, activity was controlled by the ATP-derived adenosine from glial cells, interacting with the A1 receptor on the thalamocortical neurons (Hughes et al. 2011; Lörincz et al. 2009; Parri et al. 2001; Parri and Crunelli 2001). The generation of infraslow activity may involve additional mechanisms, e.g., nonneuronal sources, including glia cells, or the blood brain barrier (Amzica and Steriade 2000; Vanhatalo et al. 2004; Voipio et al. 2003).

We study infraslow activity in patients with varying degrees of a postanoxic encephalopathy. Previously, we have shown that in these patients irreversible brain damage is associated with persistent isoelectric or severely depressed EEG activity (Cloostermans et al. 2012; Tjepkema-Cloostermans et al. 2015). In some patients, isoelectric recordings were interpuncted with stereotypical bursts, resulting in "burst-suppression with identical bursts" (Hofmeijer et al. 2014b), that may appear in clusters. We hypothesize that infraslow activity modulates cortical excitability and that these burst-clusters are phase-locked to infraslow oscillations. Our observations are supplemented with simulations of burst-suppression in the absence and presence of infraslow oscillations in a minimal mathematical model.

METHODS

Since 2011, all patients with postanoxic coma after cardiac arrest submitted to our intensive care unit (ICU) are routinely monitored with continuous EEG. EEG is recorded starting as soon as possible after patients' arrival in the ICU typically within 24 h after ICU admission and continued for 2–3 days or until discharge from the ICU. EEG monitoring is part of routine clinical care. Informed consent for recording and follow-up was waived by the institutional review board. In part, data from some patients were used in previous publications, reporting on the prognostic value of EEG in patients with a postanoxic encephalopathy (Cloostermans et al. 2012), including EEG burst-suppression with identical bursts (Hofmeijer et al. 2014b).

Full-band EEG recording. All EEGs were recorded with a Neurocenter EEG system (Clinical Science Systems) with a TMS-i DC-coupled amplifier and active shielding technology (TMS-international) using 21 silver-silverchloride cup electrodes at the standard 10/20 recording position. Sampling frequency was set to 256 Hz. Data were digitized with 24 bit but stored to disk in 16 bit EDF+ format. In 2013, we implemented the method described in Kemp et al. 2010 that allows storage of full-band (24 bits) EEG data into standard EDF+ format. All patients included in the current study had their EEGs processed by this method.

Treatment. Patients were treated according to current standard therapy, as described previously (Cloostermans et al. 2012). In short, patients were mechanically ventilated, and mild therapeutic hypothermia of 33°C was induced as soon as possible after the arrest and maintained for 24 h by intravenously administered cold saline and cooling pads. Propofol or midazolam was used for sedation to a level of −4 or −5 on the Richmond agitation sedation scale and discontinued after normothermia had been reached, if possible. Fentanyl or Remifentanil was used against shivering. In one patient therapeutic hypothermia was not possible. After sedation was stopped and normothermia was reached, treatment was discontinued if the somatosensory-evoked potential after stimulation of the median nerve was bilaterally absent. Other reasons for treatment withdrawal included insufficient neurological recovery after 4–7 days and nonneurological complications.

Clinical outcome. The primary clinical outcome measure was the best score on the cerebral performance category (CPC) within 6 mo dichotomized between "good" (CPC 1 or 2) and "poor" (CPC 3, 4, or 5). The CPC scores were assigned based on telephone interviews by an experienced investigator (M. C. Tjepkema-Cloostermans) blinded to the EEG at 3 and 6 mo. Secondary outcome measures included mortality (Cloostermans et al. 2012).

Analysis of full-band EEG. We visually classified EEG patterns in isoelectric recordings, low-voltage (<20 μV), burst-suppression with and without identical bursts, epileptiform activity, diffuse slowing, and (relatively) normal (dominant frequency ≥8 Hz and amplitudes >20 μV).

Bursts were considered identical if on visual inspection burst were identical and if the mean correlation coefficient of N subsequent bursts was larger than 0.75, as evaluated from all possible cross-correlations of the $0.5\cdot(N^2 - N)$ different bursts, setting the correlation length to 600 ms. For details, we refer to (Hofmeijer et al. 2014b).

Infraslow activity was evaluated for the whole duration of the EEG recording in a single bipolar montage F3-C3 with band-pass filter settings 0.01–0.1 Hz. Maximum amplitudes of the infraslow activity were estimated from the mean value of the envelope, using the Hilbert transform. Infraslow activity was considered present in a 10 min epoch if the mean peak-to-peak amplitude was larger than 10 μV. The average frequency of the infraslow activity was estimated from the mean value of the zero-crossings of the autocorrelation. If the standard deviation of the zero-crossings was less than 25%, we considered the infraslow activity periodic.

To quantify phase-amplitude coupling in 10 min epochs of EEG (including bursts) to infraslow activity, we use the method by Tort et al. (Tort et al. 2010). We first estimate the phase ϕ of infraslow activity, after filtering in the frequency range 0.01–0.1 Hz in steps of 0.0025 Hz with a bandwidth of 0.005 Hz, using the Hilbert transform. The mean amplitude of EEG activity is obtained from the absolute value of the Hilbert transformation, for all frequencies in the range 3–30 Hz in steps of 1 Hz with a bandwidth of 4 Hz. For each phase and frequency, we thus obtain the distribution of amplitudes as a function of the phase of the infraslow activity. In the case of significant phase dependency, the deviation of a uniform distribution of amplitudes for each frequency bin (e.g., 3–7 Hz) is quantified using the modulation index, MI, defined as

$$\mathrm{MI} = \frac{\log(N) + \sum_{i=1}^{N} A_i \cdot \log A_i}{\log(N)} \quad (1)$$

where N is the number of phase bins (similar to Tort, we set $N = 18$), and A_i with $i = 1,\cdots,N$ is the normalized amplitude of the EEG signal in a particular phase bin defined as

$$A_i = \frac{a_{\phi i}}{\sum_{j=1}^{N} a_{\phi j}} \quad (2)$$

with $a_{\phi i}$ the mean amplitude of the signal at phase ϕ_i. If all normalized amplitudes are equally distributed, MI = 0, if only one phase bin contains all the power MI is maximal with MI = 1, thus normalizing the MI in the range [0 − 1]. This procedure provides a value for the MI for each phase-frequency combination that can be visualized in a comodulogram.

Table 1. *Parameter values used in the simulations*

Parameter	Value
n	1
τ_a	1
θ_a	0.18
k_a	0.05
τ_d	2
θ_d	0.5
k_d	0.2
τ_s	700
θ_s	0.14
k_s	0.04

Statistical significance of the MI was evaluated by random assignment of $a_{\phi i}$ to each phase bin. By repeating this procedure for 100 times, we created surrogate MI, where the significance threshold was set to the maximum value of these surrogates. As the MI is based on two particular signals, we can in principle estimate significance for each combination of two band-pass filtered signals. Here, we evaluate if significant modulation was present for infraslow EEG activity in the frequency range 0.01–0.1 Hz and EEG rhythms in the frequency range 3–30 Hz for all EEGs in our data set. All calculations were performed for nonoverlapping epoch lengths of 10 min, and filtering was performed using a first order zero-phase (Butterworth) filter in Matlab using the filtfilt.m function (The Mathworks). For each epoch, we estimated the frequency and amplitude of the infraslow activity, the comodulogram and the MI.

Statistical analysis. For statistical analysis, we used R (R Development Core Team 2008). Between-group differences were evaluated with the Wilcoxon-test, *wilcox.test*, and linear regression using the function *lm*.

Modeling burst-suppression. To better understand the presumed modulation of burst-suppression patterns by infraslow activity, we use a minimal computational model to simulate burst-suppression. This model was initially proposed by Tabak et al. (Tabak et al. 2000) and describes the average activity of a neuronal population. The model consists of a fast system, with two stable states, resting or bursting, and a slow subsystem. The model generates identical bursts in an excitatory neuronal network with recurrent feedback and was also used to simulate burst-suppression in clinical EEGs from patients with postanoxic coma (van Putten and van Putten 2010).

The network is self-excitatory, where the output of the excitatory neurons, with activity a, is fed back to the cells, where the amount of feedback depends on the connectivity, n. At the synaptic level, feedback is modulated by a fast depression, d, and a slow depression, s. This results in an input current, I, to the cells in the network

$$I = a \cdot b \cdot s \cdot n. \tag{3}$$

Two equations describe the burst dynamics, i.e., the network activity, a, with time constant, τ_a, and a fast depression, d, with time constant τ_d. One equation describes the slow modulation or depression, s, with time constant τ_s. The equations are

$$\begin{aligned} \tau_a \dot{a} &= a_\infty(I) - a \\ \tau_d \dot{d} &= d_\infty(a) - d \\ \tau_s \dot{s} &= s_\infty(a) - s \end{aligned} \tag{4}$$

where the time constant $\tau_s \gg \tau_a + \tau_d$.

The steady-state activation curves a_∞, d_∞, and s_∞ are approximated by the Boltzmann functions

$$\begin{aligned} a_\infty(I) &= 1/\{1 + \exp[-(I - \theta_a)/k_a]\} \\ d_\infty(a) &= 1/\{1 + \exp[(a - \theta_d)/k_d]\} \\ s_\infty(a) &= 1/\{1 + \exp[(a - \theta_s)/k_s]\}. \end{aligned} \tag{5}$$

The values of k_x with $x \in a, d, s$ define the steepness of the sigmoid, while at values θ_x with $x \in a, d, s$ half-activation occurs, since $x_\infty(\theta_x)$. If the network shows high (low) activity, the variables d and s decrease (increase).

The slow system that induces the depression s essentially shifts the fast subsystem from one state to the other periodically, resulting in a burst-suppression pattern. At which value of s the bifurcations occur depends on the steady-state activation curves of the fast subsystem.

We now add a slow external sinusoidal current to the network that represents an infraslow oscillation (ISO), resulting in a total current $I_{tot,}$ given by

$$I_{tot} = a \cdot d \cdot s \cdot n + \underbrace{S \cdot \sin(2 \cdot \pi \cdot t/T)}_{\text{ISO}} \tag{6}$$

with S the amplitude of the modulating sinusoidal current and T the period. We subsequently study the effect of this external current on the occurrence of the bursts, by replacing I in *Eq. 3* with $I_{tot,}$ The amplitude S of the imposed current was less than 10% of the total effective current, I_{tot}. Parameter values were similar to the values used by Tabak et al, and are presented in Table 1. The model equations were implemented within XPPAUT (freely available software by G. B. Ermentrout, http://www.math.pitt.edu/~bard/xpp/xpp.html), setting the time step $dt = 0.2$. For further details we refer to (Tabak et al. 2000; van Putten and van Putten 2010).

RESULTS

Full-band EEG recordings from all 41 patients were included. Continuous EEG monitoring was started at a median of 10 h (interquartile range 11.7 h, range 2.5–76 h) after cardiac arrest. Fifteen patients (37%) had a good outcome. All patients with a poor outcome died. Characteristics of the included patients are summarized in Table 2.

Incidence of infraslow activity. Infraslow activity defined as EEG activity in the 0.01–0.1 Hz range with peak amplitudes larger than 5 μV was present in all postanoxic patients, irrespective of outcome. The durations varied, with an average of 88% of the recording time. Maximum amplitudes of the infraslow activity ranged from 5 to 150 μV and were, on a group level, not statistically significantly different between patients with poor and good outcome ($P < 0.11$). However, maximum amplitudes larger than 35 μV were only observed in

Table 2. *Baseline characteristics, cause of cardiac arrest, and treatment*

Patients, *n*	41
Men, *n*	28 (68.3%)
Good neurological outcome	15 (36.6%)
Age, yr	59.6 ± 13.4
OHCA	33 (80.5%)
Initial rhythm	
VF	20 (48.8%)
Asystole	15 (36.6%)
Bradycardia	1 (2.4%)
Unknown	5 (12.2%)
Propofol treatment	40 (97.6%)
Propofol dosage, $mg \cdot kg^{-1} \cdot h^{-1}$	3.0 ± 1.0
Midazolam treatment	9 (22.0%)
Midazolam dosage, $\mu g \cdot kg^{-1} \cdot h^{-1}$	67.1 ± 32.6
Fentanyl treatment	28 (68.3%)
Fentanyl dosage, $\mu g \cdot kg^{-1} \cdot h^{-1}$	1.6 ± 0.7
Remifentanil treatment	13 (31.7%)
Remifentanil dosage, $\mu g \cdot kg^{-1} \cdot h^{-1}$	5.3 ± 3.1

Data are presented as number (%) or means ± SD. OHCA, out of hospital cardiac arrest; VF, ventricular fibrillation; dosage indicates maximum dosage within the first 24–48 h.

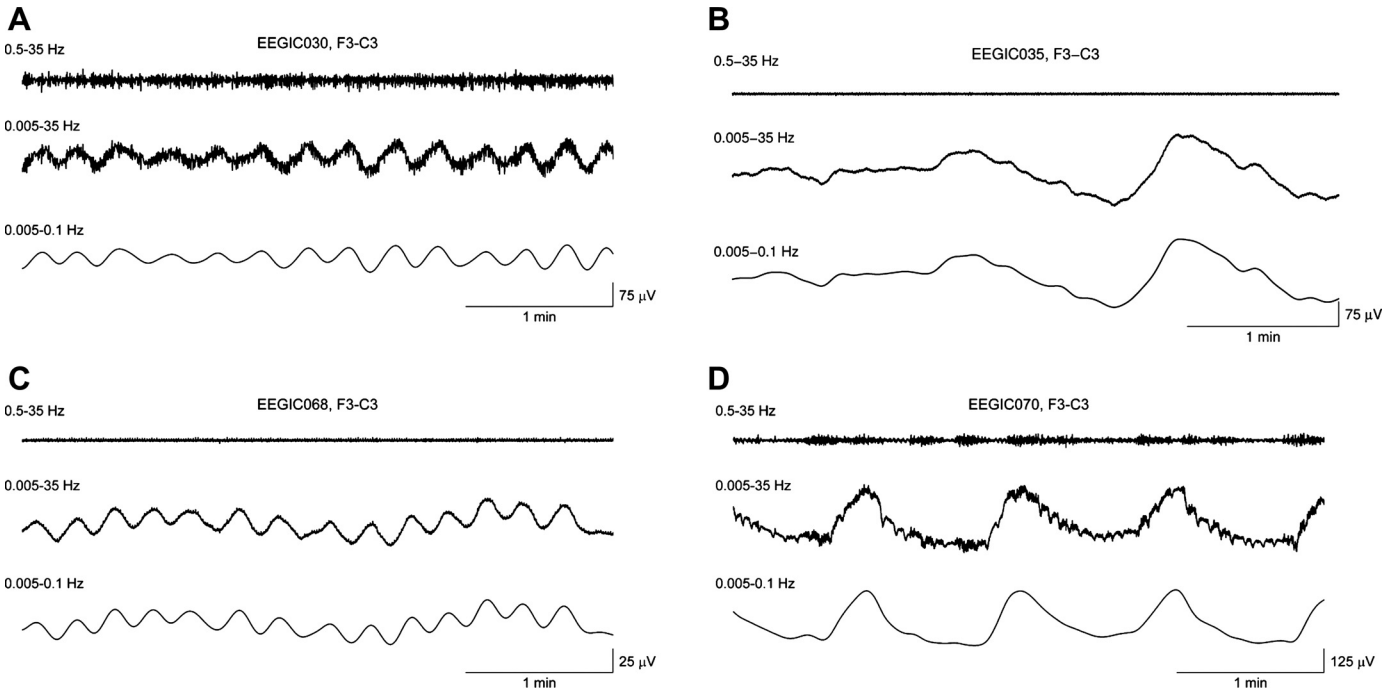

Fig. 1. Four examples (*A–D*) of infraslow activity in patients with postanoxic coma. We used 3 different filter settings: 0.5–35, 0.005–35, and 0.005–0.1 Hz. Infraslow activity ranges from ≈0.01 to ≈ 0.1 Hz. Note the small amplitude of activity at frequencies $f > 0.5$ Hz in *B* and *C*, where the EEG with conventional filter settings is nearly isoelectric, but infraslow activity is preserved, with amplitudes up to 150 μV.

patients with poor outcome. Infraslow activity was in the frequency range 0.015–0.06 Hz, similar for both groups ($P < 0.31$). Examples are presented in Fig. 1. Note the very small amplitude of the EEG with conventional filter settings in Fig. 1, *B* and *C*, while infraslow activity is preserved, with amplitudes up to 150 μV. In many recordings, infraslow activity was temporarily periodic, resulting in infraslow oscillations. Two examples of the time course of the amplitude and frequency of infraslow activity are presented in Fig. 2.

Phase-amplitude coupling. Phase-amplitude coupling between the infraslow activity and EEG rhythms in the frequency range 3–30 Hz was estimated in all patients. In most patients with good (13/15) or bad (20/26) outcome, the MI was significant during the first 48 h after resuscitation, but durations of modulation varied from one to several hours. Although no group differences were found for the maximum values of the MI ($P < 0.27$), the maximum value for the MI in patients with good outcome was MI = 0.016. In all patients with MI >

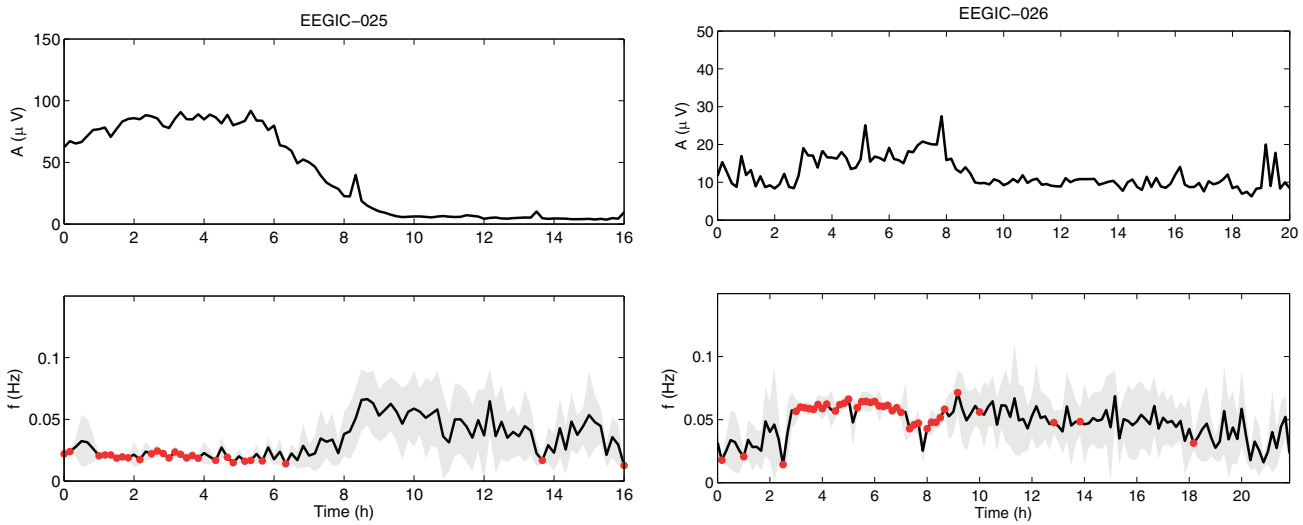

Fig. 2. Temporal evolution of infraslow activity in 2 patients. *Left*: illustrative example of the time-course of infraslow activity (ID025). *Top*: amplitude of the infraslow activity, with initial values up to 100 μV. *Bottom*: frequency of the infraslow activity. The gray-shaded area indicates ± 1 SD. The red dots are the moments when the infraslow activity (f ≈ 0.025 Hz) was considered periodic (change in frequency during 10 min epoch <25%). Start of the recording is 14 h after cardiac arrest. This patient had a poor outcome. *Right*: infraslow activity of patient ID026. The amplitude of the infraslow activity is 10–25 μV. In particular between 3 and 8 h infraslow activity is periodic with a frequency of ~0.06 Hz. Start of the recording 13 h after cardiac arrest. This patient recovered well.

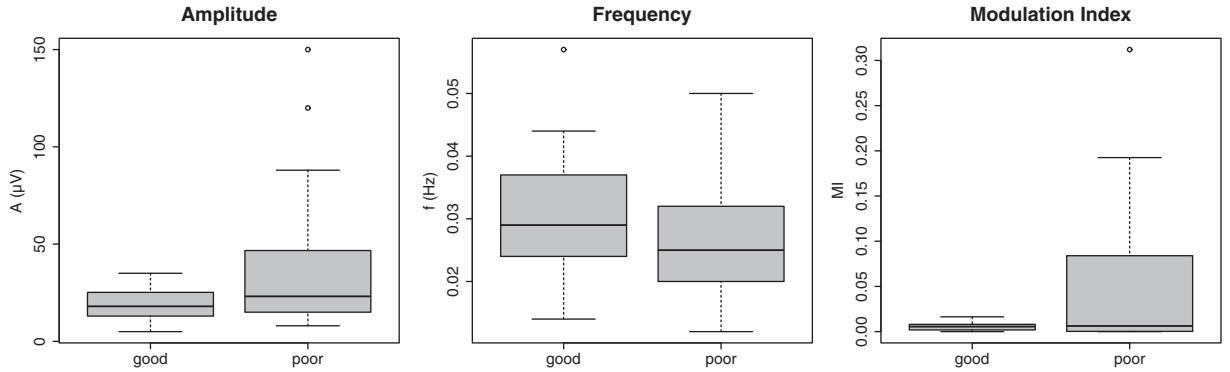

Fig. 3. Boxplots of amplitudes and frequency of infraslow activity and the modulation index (MI). Boxplots [median, 1st, and 3rd quartile, whiskers show minimum and maximum (without outliers) and outliers, indicated with ○] of maximum amplitudes of the infraslow activity observed during the recording interval, the mean frequency of the infraslow activity, and maximum values of the MI. Good, good outcome [cerebral performance category score (CPC) = 1 or 2]; poor, poor outcome (CPC = 3, 4 or 5). Differences between groups of patients with good and poor outcome were not statistically significant. However, in patients with amplitudes of the infraslow activity >35 μV or MI >0.016, outcome was invariably poor.

0.016 [11/26 (42%)], outcome was poor. There was no correlation between the maximum amplitude of the infraslow activity and the MI in patients with a good outcome ($R = 0.0001$, $P > 0.9$), whereas a modest, but statistically significant, correlation in patients with a poor outcome was found ($R = 0.59$, $P < 0.01$). Maximum amplitude and frequency of the infraslow activity and the MI are further summarized in Fig. 3.

Infraslow activity and burst-suppression with identical bursts. We identified 14 patients (34%) showing burst-suppression with identical bursts. EEG patterns often evolved from low-voltage or isoelectric EEG recordings, as exemplified in Fig. 4. Burst-suppression with identical bursts was invariably a transient pattern, with duration of 1.5–22 h, changing to burst-suppression without identical bursts, generalized periodic discharges or diffuse slowing.

In nine patients, bursts were phase-locked, where the maximum value of the MI ranged from 0.02 to 0.31. In these patients, infraslow activity was periodic for several hours (except in *patient 047*, where periodicity was limited to 10–20 min), resulting in infraslow oscillations. In these patients, the bursts appeared as clusters. Additional details of these patients are shown in Table 3. Four examples of the time-series are presented in Fig. 5. The inserts show details of the bursts that have identical shapes. In five patients, bursts were not clustered and infraslow activity was not periodic.

In patients with burst-suppression with identical bursts and phase-locking of bursts to infraslow activity, phase-locking was always a transient phenomenon, present for several hours. The temporal evolution of EEG activity in a patient with burst-suppression with identical bursts is illustrated in Fig. 6, together with three exemplary comodulograms and corresponding values of the MI.

Simulations. We assessed if the introduction of a slow oscillatory current in a minimal computational model for burst-suppression with identical bursts could induce clustering of bursts. The model, without an external current, generates burst-suppression patterns where the bursts are identical and appear regular, as reported previously (Tabak et al. 2000; van Putten and van Putten 2010). The slow subsystem induces the depression, s, that shifts the fast subsystem, responsible for burst-generation, from one state to the other, i.e., bursting or not: if the value of s becomes sufficiently large, bursting starts, and when it becomes sufficiently small, bursting ends (Fig. 7, *top middle*).

During the interburst interval, the period of low activity, there is a slow increase of s and a, while d will slightly decrease, where the change of a and d are at the same pace of

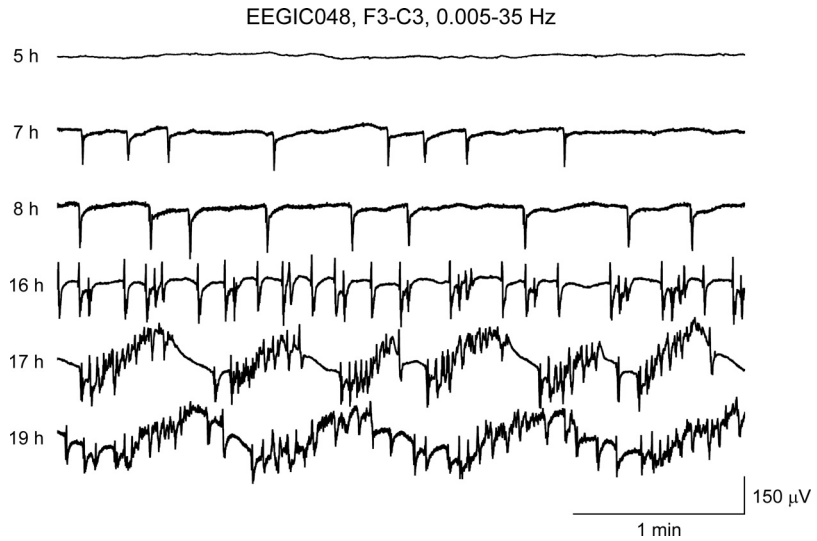

Fig. 4. Example of temporal evolution of burst-suppression pattern with identical bursts. The time of each trace is given in respect to the time of cardiac arrest. There is a gradual appearance of bursts and infraslow activity, evolving to infraslow oscillations, with a period of approximately one min at $t = 19$ h. Clusters of bursts are most apparent at $t = 17$ h, phase-locked to the up-slope of the infraslow activity.

Table 3. *Overview of start of the EEG recording, the emergence (relative to time of cardiac arrest) and duration of the infraslow activity in 9 patients with burst-suppression with identical bursts that were strongly phase-locked with MI ≥0.02 to infraslow oscillations, resulting in burst clusters*

ID	start EEG, h	Emergence, h	MI_{max}	Dur, h	f_{ISA}, Hz	A_{ISA}, μV	Propofol, $mg \cdot kg^{-1} \cdot h^{-1}$
025	14	14	0.08	7	0.02	90	3
029	16	20.5	0.13	2.5	0.02	120	3.7
035	4	5	0.10	4	0.03	25	2
041	16	19	0.08	1	0.03	15	2.3
043	11	16	0.08	22	0.04	50	4.8
047	9	27	0.02	14	0.03	20	2.2
048	4.5	24	0.15	10.5	0.02	75	2.7
050	17	17	0.12	1.5	0.02	40	3.3
071	10	13	0.31	6	0.01	150	4

One patient (025) was not treated with mild therapeutic hypothermia; another patient (047) also had a traumatic brain injury. MI, modulation index; Dur, duration; f_{ISA}, frequency of the infraslow activity; A_{ISA}, maximum amplitude of the infraslow activity.

s because the time constant $\tau_d + \tau_a \gg \tau_s$. The actual values of s that determine the initiation or the ending of bursting are defined by the steady-state activation curves of the fast subsystem. The bifurcation diagram is shown in Fig. 8, and the hysteresis loops are shown in Fig. 9. By adding a small external oscillatory current, bursts appear in clusters, which are correlated with the phase of the external current. These two simulations are illustrated in Fig. 7, *bottom*.

Phase-locking to the external input essentially results from slowly changing the threshold for which the self-excitatory input to the network, $I = n \cdot s \cdot d \cdot a$, results in bursting or not, which mainly depends on s. Therefore, the external current changes the regime of s where bursting occurs. A negative current shifts the regime upward, while a positive current produces the opposite effect. As the thresholds for bursting have become variable now, defined by the phase of the external current, clusters of bursts can appear, as shown in Fig. 7, *bottom*. In this example, bursts cluster in triplets, where the burst duration and number of phases per burst gradually shortens from six to four (Fig. 9, *bottom right*).

DISCUSSION

Using full-band EEG recordings we show that infraslow activity is preserved in patients with postanoxic coma after cardiac arrest. In most patients, power of the EEG in the frequency range 3–30 Hz was modulated by the infraslow activity for variable durations in the first 48 h after cardiac arrest, quantified with the MI. In patients with burst-suppression with identical bursts, we often observed burst clusters that were correlated with the phase of the infraslow oscillations. We simulate this phenomenon in a minimal computational model, using a slowly varying external current as the infraslow

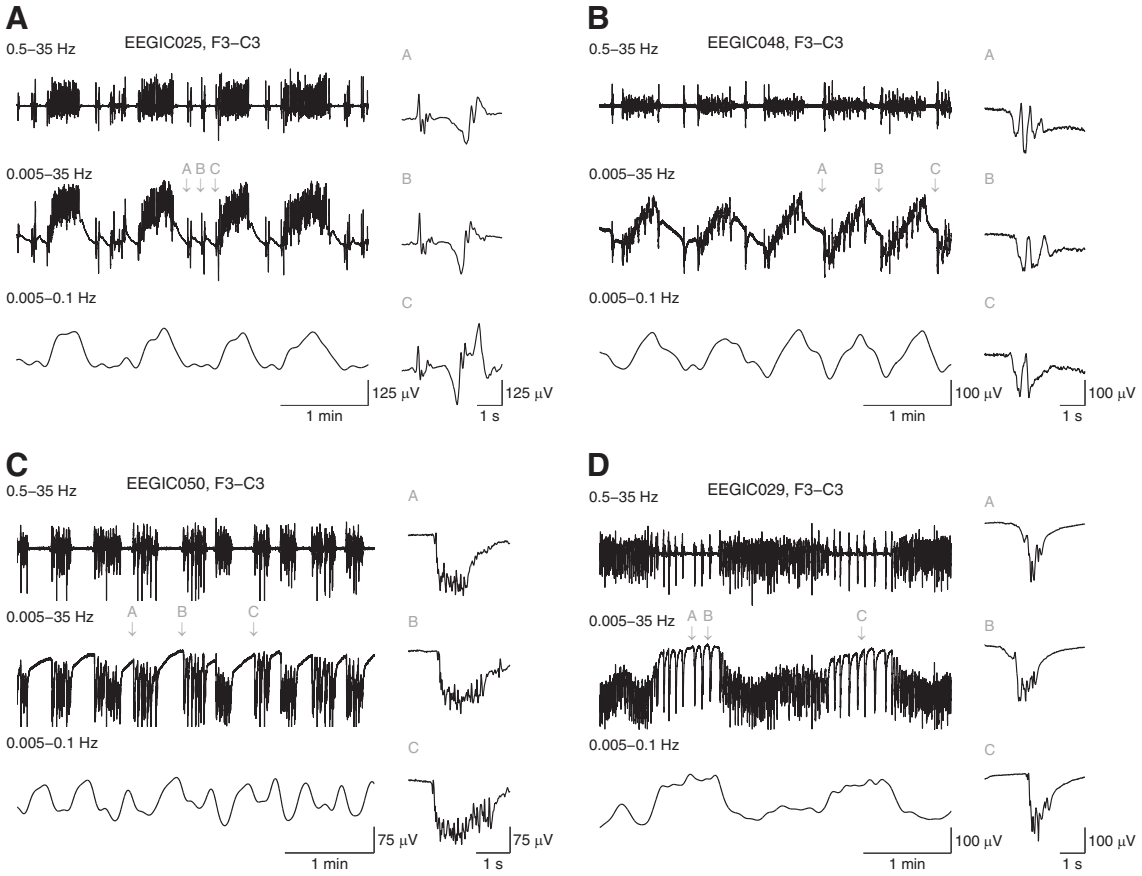

Fig. 5. Examples of burst clusters and infraslow activity. Four examples, *A–D*, of burst-suppression patterns with identical bursts in postanoxic patients, where the burst frequency is correlated with the phase of the slow oscillations, resulting in clusters of identical bursts. We used 3 different filter settings: 0.5–35, 0.005–35, and 0.005–0.1 Hz. Infraslow activity ranges from ≈ 0.01 to ≈ 0.05 Hz. *Right* subpanels: 3 individual bursts; in each patient, bursts are nearly identical. Note, that in *patients A* and *B*, bursts cluster at the up-slope of the infraslow oscillation, and in *patients C* and *D* at the down-slope.

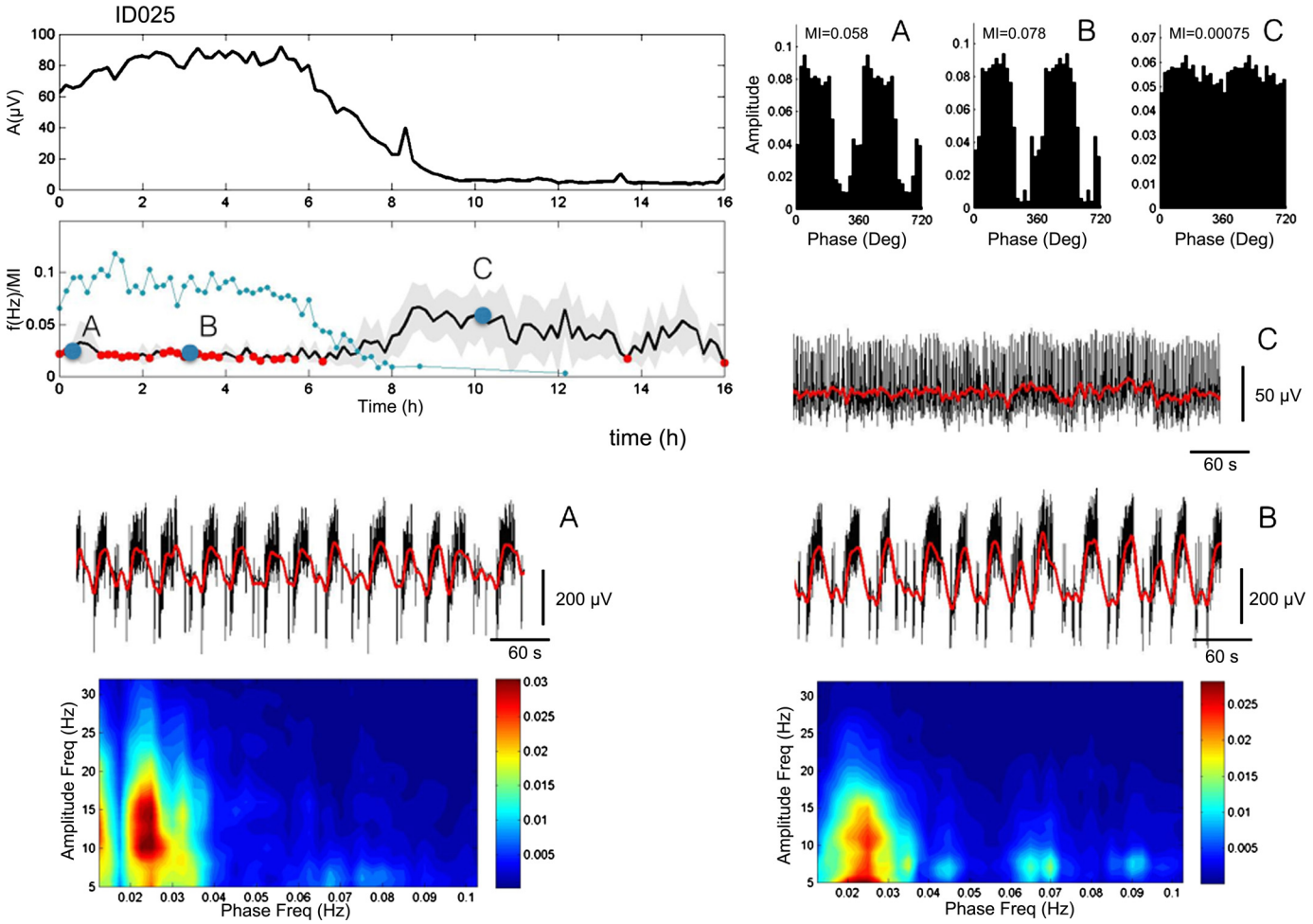

Fig. 6. Dynamics of infraslow activity, comodulogram, and MI in a patient with burst-suppression with identical bursts. Left two top panels show the time course of the frequency and amplitude of infraslow activity in a patient with burst-suppression with identical bursts. In the bottom panel of these two, the line with the small light blue dots represents the values of significant modulation quantified with the MI. The three histograms, *A–C*, show the distribution of the amplitudes as a function of the phase of the infraslow activity with MI = 0.058, 0.078, and 0.0075, respectively. To assist in the visual interpretation, two phase cycles are shown. The three corresponding time signals are shown as well, where the infraslow activity is indicated with the red line. The two comodulograms show strong modulation at ~0.025 Hz at t = 0:30 h and 3:10 (indicated with the large blue filled circles in the bottom of the two panels at top left). Initially, infraslow activity is periodic (small red dots), and there is a strong phase synchronization with the bursting activity, resulting in burst clusters, that gradually disappears. This patient died.

activity. These observations suggest that infraslow activity modulates cortical excitability. The strongest modulation is observed in patients with a severe postanoxic encephalopathy and burst-suppression with identical bursts.

Infraslow activity is preserved in postanoxic encephalopathy. In all patients with postanoxic coma, we were able to record infraslow activity, irrespective of outcome, with frequencies of 0.015–0.06 Hz and amplitudes from 5 to 150 μV. We remark that in some of the patients with low amplitude EEG (5–15 μV, see e.g., Fig. 1*C*), we cannot completely exclude spurious detection of infraslow activity due to narrow band filtering. However, this will not result in periodic infraslow oscillations, given the bandwidth of our filter.

In several patients, infraslow activity gradually appeared several hours after cardiac arrest (cf. Fig. 4), probably reflecting transient hypoxic/ischemic synaptic arrest (Hofmeijer and van Putten 2012; Hofmeijer et al. 2014a; Murphy et al. 2008; van Putten 2012). Infraslow activity with amplitudes larger than 35 μV was always associated with burst-suppression with identical bursts and poor outcome.

In all patients, infraslow activity was temporarily periodic with variable durations of 5–40% of the recording time in the first 24–36 h after cardiac arrest. Although rhythmic infraslow activity has been recorded from thalamic slices under experimental in vitro conditions, periodic infraslow activity has, to our knowledge, not been reported previously in humans. For example, in Vanhatalo et al. (Vanhatalo et al. 2004), infraslow activity (Fig. 3 in their paper) is more irregular. Also, infraslow activity from human BOLD and EEG studies lacks periodicity (Hughes et al. 2011). The mechanism responsible for the (transient) periodicity of the infraslow activity in patients with postanoxic encephalopathy is presently unclear.

In two patients, we recorded infraslow activity, while EEG rhythms with frequencies >0.5 Hz were absent. Faster EEG activity results from oscillatory postsynaptic currents generated by intracortical connections, while infraslow oscillations likely involves inputs from subcortical structures (Vanhatalo et al. 2004), although nonneuronal sources, e.g., glia, may be involved as well (Amzica and Steriade 2000). This observation, therefore, may result from selective damage to cortico-cortical

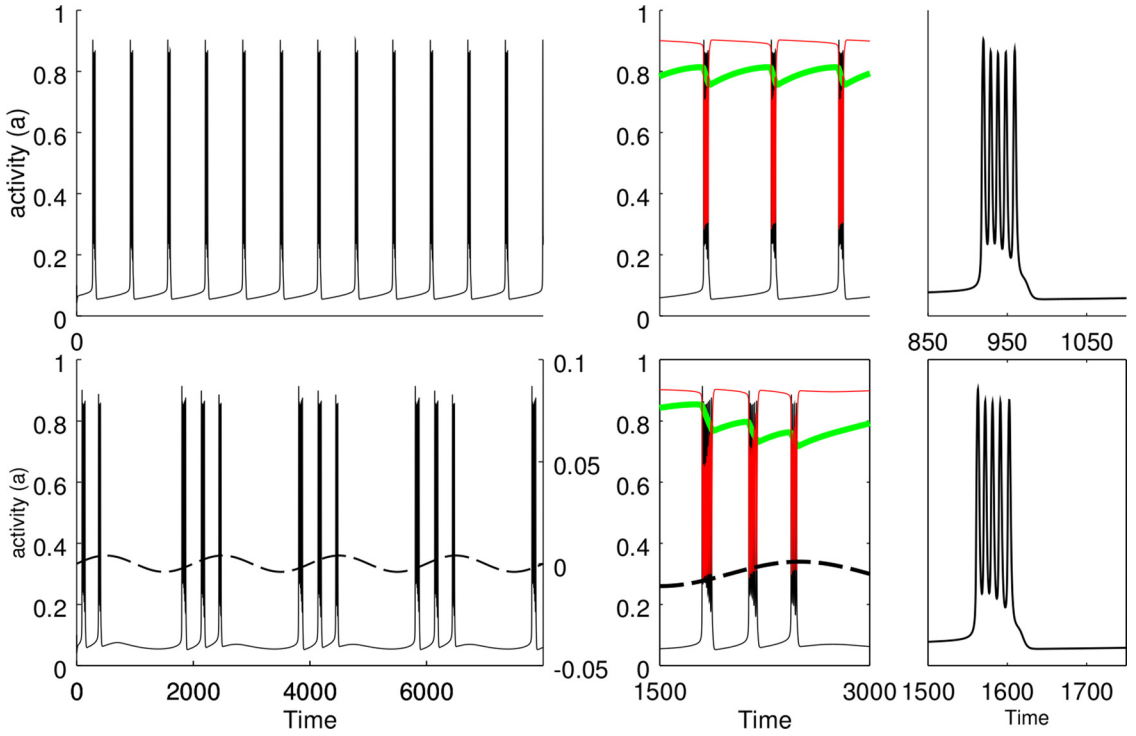

Fig. 7. Burst suppression generated by the model. *Top left*: bursts appear regular and are not clustered. Burst shapes are identical (see two right panels, where two consecutive bursts are shown). *Bottom left*: phase-locking of bursts to an infraslow oscillation (dashed line, with period $T = 2{,}000$), resulting in clustering of the bursts. Note that the locking is asymmetrical, where bursts are mainly locked on the up-going slope of the oscillatory current, similar to several of our observations. The middle panels show details of the activity with the slow modulation s (green) and the fast depression, d (red). The amplitude of the modulating current was set to $S = 0.004$ (dashed curve). Time is in arbitrary units.

synapses, with preservation of thalamocortical synapses presumably relaying infraslow oscillatory input from thalamic relay nuclei (Hughes et al. 2011).

This possible dissociation of primary cortical and subcortical activity is in line with our previous observation of preserved thalamocortical input as expressed by preservation of the early response (N20) of the somatosensory evoked potential, in the absence of spontaneous EEG activity (van Putten 2012). The main contribution to the N20 is the extracellular current generated by the excitatory (non-NMDA) postsynaptic currents from pyramidal cells receiving synaptic input of the thalamocortical cells (Castro-Alamancos and Connors 1997). Conditions exist where these postsynaptic currents are preserved and sufficiently large to be recorded on the scalp, while synapses emerging from pyramidal cells, involved in the generation of primary cortical rhythms, are silent.

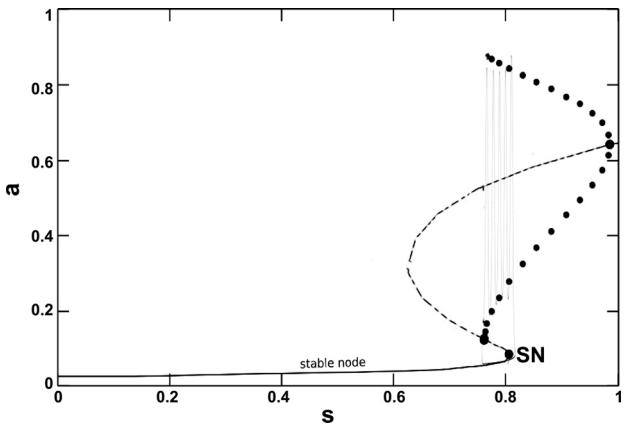

Fig. 8. Bifurcation diagram. Shown is the bifurcation diagram of the fast subsystem with s as a bifurcation parameter. As s approaches $s = 0.81$, a saddle node (SN) bifurcation if reached, and bursting will start. During this period, the mean activity of a is increased, and therefore s will be slowly suppressed. Spiking will halt when the limit cycle disappears. The solid line indicates stable equilibria, the thin dashed curve unstable equilibria, where oscillations (stable limit cycle, representing the bursts) occur. The dotted line shows the approximate amplitude of the bursts around the unstable steady states. A burst is indicated (cf Fig. 9, left bottom panel).

Similar observations of this differential sensitivity of subcortical and cortical signals after global hypoxic ischemia were recently reported after induction of cardiac arrest in a rodent model (Wu et al. 2012). Evoked neuronal activities were recorded from the primary somatosensory cortex. Long latency responses disappeared first, while short latency responses (similar to the N20) disappeared later. Hereafter, a period of isoelectric silence occurred, followed by reappearance of the short latency response prior to the long latency response. As the long latency response primarily reflects cortical activity, the authors conclude that cortical activity is more vulnerable to ischemic injury than subcortical activity. This selective ischemic vulnerability may result from differences in metabolic demands or mitochondrial reserves. Thalamocortical relay neurons, for instance, are 10 times as energy efficient as cortical neurons (Moujahid et al. 2014).

Modulation of EEG rhythms by infraslow activity. In most patients, either with good (13/15) or poor outcome (20/26), modulation of the power in the frequency range of 3–30 Hz with infraslow activity (0.01–0.1 Hz) is observed at some period during the first 48 h after cardiac arrest. Although on group level, no differences were found between the MI and the

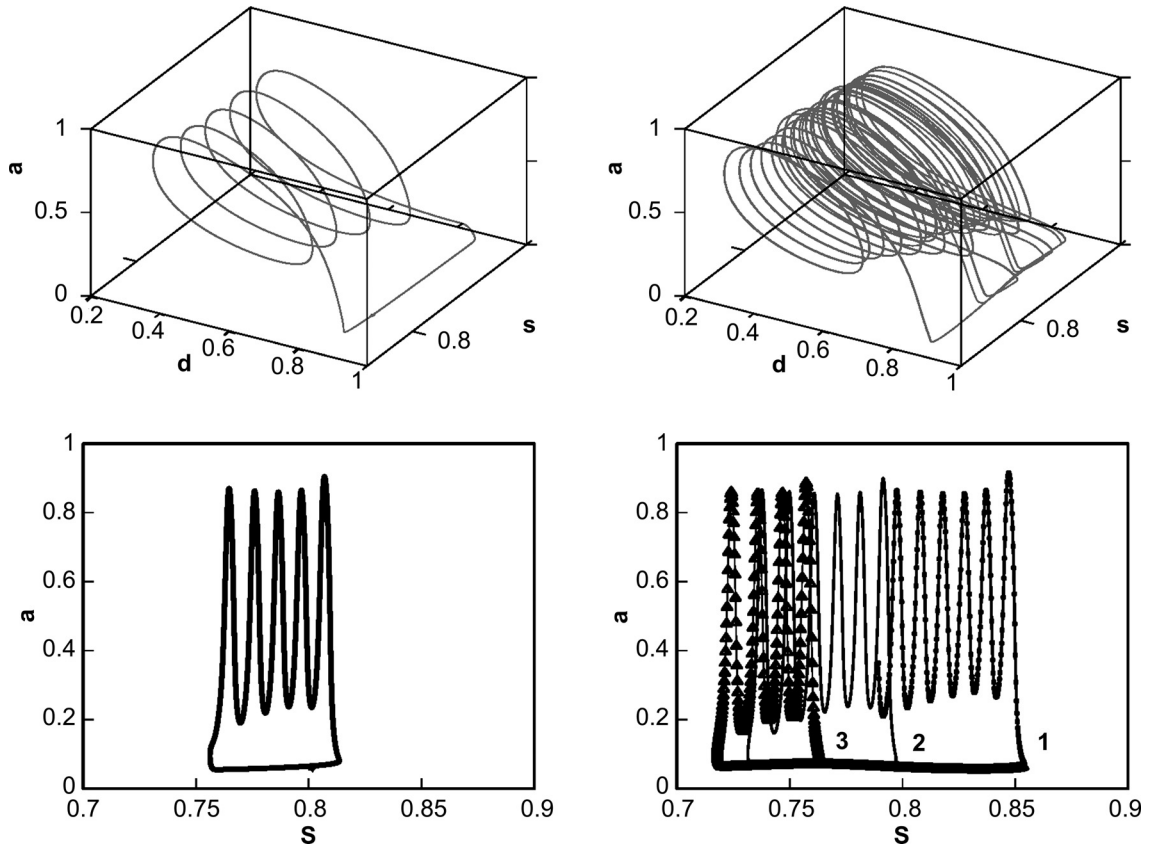

Fig. 9. Hysteresis loops and projections of the slow system. *Top*: hysteresis loops for the model without (*left*) and with an external current (*right*). *Bottom*: the 2D projections with the slow system, s on the x-axis and activity, a, on the y-axis. The initiation of the bursts in the bottom right panel is indicated with 1, 2, and 3. The range of values of s were bursting occurs is larger with the external current. While bursting starts at a value of $s = 0.81$ without an external current, it starts at values $s = 0.86$ with a negative current. Similar, bursting stops at values $s = 0.76$ without an external current, while it ends at varying values, with a minimum at $s = 0.71$, where the positive current injection is at its maximum. After the burst period ends, s slowly increases to its value where bursting starts again. The change needed to start bursting again is much larger with the external current than without, with $\Delta s = 0.15$ vs. $\Delta s = 0.05$, respectively.

duration of modulation, values of the MI in patients with a good outcome never exceeded MI = 0.016. Large values of the modulation [MI = (0.02–0.31)] and associated large amplitudes of the infraslow oscillations (cf. Table 3) were only observed in patients with burst-suppression with identical bursts, as will be discussed next. The relatively small values of the MI result from the definition of the MI: a value MI = 1 reflects the presence of EEG power in a particular frequency in a single phase bin only (cf. *Eq. 1*). This was never observed in our data, showing nonzero EEG power at each phase bin. This may result in relatively low values of the MI that may still reflect significant modulation. Similar MI values are reported in Tort et al. (Tort et al. 2010).

Burst clusters in burst-suppression with identical bursts may result from phase-locking to infraslow oscillations. Burst-suppression is an EEG pattern characterized by high amplitude events (bursts), alternated by periods of low or absent activity (suppressions; amplitudes < 10 μV). EEG burst-suppression occurs in various circumstances, ranging from prematuritas or anesthesia to severe pathology, including postanoxic encephalopathy (Cloostermans et al. 2012). Mechanisms responsible for burst-suppression vary and may involve the inactivation of inward currents or the activation of outward currents, which may be voltage or Ca^{2+} gated (Hofmeijer et al. 2014b; Izhikevich 2007; Liley and Walsh 2013; van Putten and van Putten 2010).

Recently, we identified a subtype of burst-suppression EEG with bursts showing extreme stereotypy: burst-suppression with identical bursts, exclusively present in patients with a severe postanoxic encephalopathy and invariably associated with a poor outcome (Hofmeijer et al. 2014b). Here we show that in a large fraction (57%) of these patients bursts are clustered, and phase-locked to infraslow oscillations, as illustrated in Figs. 5 and 6.

Bursts are relatively discrete events, and to quantify phase-locking, we could have implemented a method to determine the phase relationship of the time of occurrence of individual bursts. However, the power of the EEG in the 3–30 Hz range is also strongly increased during bursting, as can be appreciated from e.g., Fig. 6. This motivated us to quantify phase-locking using the technique proposed by Tort et al. (Tort et al. 2010).

The correlation found, as expressed by the MI, between the phase of the infraslow oscillations and the burst clusters, does of course not imply a causal relationship. However, we assume that burst-clustering is a result of the infraslow activity. This is in agreement with other recent literature that shows that infraslow activity is a modulator of cortical excitability (Hiltunen et al. 2014; Picchioni et al. 2011).

In disagreement with earlier observations we found that bursts were clustered either on the up-going or on the down-going slope of the infraslow oscillation. For instance, the phase

relationship between infraslow activity and faster EEG oscillations reported by Vanhatalo et al. (Vanhatalo et al. 2004) shows a symmetrical distribution around phase π, while this appeared asymmetrical in the appearance of K-complexes and interictal discharges. In the recording of the fast oscillations that were phase-locked to the infraslow 0.1 Hz activity from the neocortex of rabbit, this asymmetry is also present (Aladjalova 1957). Our simulations provide a plausible explanation for this asymmetry, as the "direction" of the external current (being either excitatory or inhibitory) defines if the range where bursting continues is enlarged or diminished. From the phase of cortical EEG we cannot deduce if the current in the underlying cortex is excitatory or inhibitory, as we have no detailed information about the relative orientation of the cortical structure and our (bipolar) electrode positions. Therefore, phase-locking could be either to an up-slope or a down-slope of the infraslow activity, as either may represent an excitatory current.

As shown in Fig. 5, there appears to be a relation between the maximum burst frequency and the minimum burst frequency: in panels Fig. 5, *A* and *D*, the maximum burst frequency is larger than in Fig. 5*C*, where in the less active states the burst frequency is reduced to nonzero values in Fig. 5, *A* and *D*, but bursts are absent at the peaks of the infraslow activity in Fig. 5*C*. As the infraslow activity is proposed to modulate the bursts, relatively low maximum frequencies may indeed be accompanied by absence of bursts. We were also able to simulate these scenarios using slightly different connectivity values (e.g., by reducing $n = 1$ to $n = 0.96$) or by using a block-pulse shaped modulating current with a nonzero, positive mean (results not shown).

Simulations. A common element in burst-suppression is the presence of at least two processes with different time scales. The first, a relatively fast process, generates the bursts, while the other, with a longer time scale, terminates the bursts and defines the duration of the interburst interval (Izhikevich 2007). In the model we used for the simulations, the fast process was represented by the network activity a, with time constant τ_a and the fast depression, d with time constant τ_d. The slow modulation was represented by s, with time constant τ_s, with $\tau_s \gg \tau_a + \tau_d$.

In the model, bursts emerge from the deactivated state (low value of a). This interburst period with low activity could represent a hyperpolarized state, e.g., resulting from an increase in potassium conductance. An experimental study in anesthetized cats in which the investigators used intracellular recordings from cortical, thalamocortical, and reticular cells showed that phasic depolarizing events were associated with bursts in the EEG, whereas the membrane potential hyperpolarized in the interburst periods (Steriade et al. 1994).

A variation of the current model could include a variable threshold for cell firing, rather than an activity dependent slow modulation s. Using a variable threshold, the threshold would slowly increase during bursting, eventually terminating the bursts, after which the threshold could recover to its initial value and bursting would start again. In fact, these two mechanisms were extensively discussed in the paper by Tabak (Tabak et al. 2000), where such model was introduced. Various other models for burst-suppression have been proposed, too, including mesoscopic models that contain much more biological detail and realistic timescales, but typically at the expense of many (20–50 or even more) parameters that need to be defined (e.g., Liley and Walsh 2013).

The main motivation for the current model is its relative simplicity and the desire to propose a potential mechanism for burst clustering. The model simulates a key characteristic of our observations, i.e., phase-locking of the identical bursts to the infraslow oscillations by adding a small external slow oscillatory current to the neuronal population, as presumed (subcortical) input as source of the infraslow activity, to induce the phase-locking of the identical bursts. The phase-locking results from a varying shift in threshold for initiating and ending the bursting of the fast subsystem.

The MI in patients with a poor outcome was also correlated with the maximum amplitude of the infraslow activity. This observation further supports the presumed changes in cortical excitability by the infraslow activity: larger amplitudes of the slow activity result in stronger phase-locking of faster EEG activity, including bursts. Larger amplitudes S of the modulating current in the model (cf. *Eq. 6*) also increase clustering and induce stronger modulation (results not shown).

In this model, in the case of burst clustering, the subsequent bursts also decrease in duration (cf. Fig. 9). Although this was observed in some of our patients, this was not invariably the case. Most likely, therefore, additional modulators exist as well.

Relationship of findings to prognosis. Although we also report on differences of the infraslow activity between patients with poor and good outcome, using amplitude, frequency of the infraslow activity, and phase-locking with faster EEG activity, this was not the focus of this study. The primary goal was to explore if infraslow activity was present in patients with a postanoxic encephalopathy and to further our understanding of burst clusters in patients with burst-suppression with identical bursts. At present, EEG features as reactivity, amplitude, continuity, dominant frequency, and characteristics of the burst-suppression patterns have shown to be strongly predictive of outcome in patients with postanoxic encephalopathy (Cloostermans et al. 2012; Hofmeijer et al. 2014b; Rossetti et al. 2010; Tjepkema-Cloostermans et al. 2015). Although amplitudes of the infraslow activity larger than 35 μV or a MI > 0.016 were always associated with poor outcome, we did not explore if these features have additional diagnostic value; this will be the topic of a future study.

Limitations. A potential limitation of our findings is that patients received sedation with propofol in the period that EEG recordings were obtained. However, isoelectric, low voltage, or burst-suppression with identical burst patterns cannot be solely induced by propofol. Propofol-induced EEG changes are well known. In the (constant) dosages that were used in our patients, the EEG mostly remains continuous, with anteriorization of the alpha rhythm (Hindriks and van Putten 2012). Furthermore, if burst-suppression is induced by propofol, bursts are heterogeneous and appear and disappear gradually (Kusters et al. 1998; Reddy et al. 1992), whereas our identical burst-suppression patterns are all characterized by flat interburst intervals and abrupt transitions between bursts and suppressions (Hofmeijer et al. 2014b). Furthermore, burst-suppression with identical bursts has also been observed in patients without sedation (Hofmeijer et al. 2014b; Hughes 1986; van Putten and van Putten 2010), and the mechanisms for their generation is most likely very distinct from propofol-induced burst-suppression

(Hofmeijer et al. 2014b; Liley and Walsh 2013). To what extent propofol may have modulated or even generated the infraslow activity cannot be deduced from our data. However, it is known that infraslow activity is present in nonsedated patients and healthy volunteers (Vanhatalo et al. 2004), and the frequencies we observe are in the same range as observed in these studies. Also, the temporal evolution of the infraslow activity, most pronounced in our patients with a severe postanoxic encephalopathy, as reflected by the periodicity and relatively high amplitudes of the infraslow activity, suggests a significant contribution of neuronal damage and partial repair, as in these periods propofol dosages were constant.

Another limitation may seem that our patients were treated with mild therapeutic hypothermia, with a target temperature of 33°C. Although brain states are temperature dependent (e.g., Whitten et al. 2009) and EEG activity vanishes if the brain temperature drops below 22–25°C (Kochs 1995), hypothermia to a level of 33–34°C produces only marginal alterations in the EEG without changes in amplitude (FitzGibbon et al. 1984). Indeed, the single patient who was not treated with mild therapeutic hypothermia (ID025) also showed burst-suppression with identical bursts and infraslow activity, similar to patients with these EEG patterns who were treated with mild therapeutic hypothermia.

Conclusion. We show that infraslow activity is preserved in patients with postanoxic encephalopathy, with frequencies ranging from 0.015 to 0.06 Hz. Infraslow activity with amplitudes >50 μV is only observed in patients with poor outcome. In both patient groups, we observed modulations of faster EEG rhythms to infraslow activity. In a large fraction of patients with burst-suppression with identical bursts, bursts showed strong phase-locking [MI = (0.02–0.31)] to infraslow oscillations, resulting in burst clusters. Our data and simulations support the notion of a subcortical generator of the infraslow activity that modulates cortical excitability, where the strongest modulation is observed in patients with severe postanoxic encephalopathy and burst-suppression with identical bursts who show burst clusters.

ACKNOWLEDGMENTS

We thank the EEG technicians of the Department of Clinical Neurophysiology of the Medisch Spectrum Twente for assistance in the EEG measurements and the ICU personnel for support. Liesbeth Wijers assisted in the simulations. Dr. Adriano Tort kindly provided the code for computing the MI and the comodulogram.

DISCLOSURES

M. J. A. M. van Putten is cofounder of Clinical Science Systems.

AUTHOR CONTRIBUTIONS

M.J.A.M.v.P., M.C.T.-C., and J.H. conception and design of research; M.J.A.M.v.P., M.C.T.-C., and J.H. performed experiments; M.J.A.M.v.P. and M.C.T.-C. analyzed data; M.J.A.M.v.P., M.C.T.-C., and J.H. interpreted results of experiments; M.J.A.M.v.P. prepared figures; M.J.A.M.v.P. and J.H. drafted manuscript; M.J.A.M.v.P., M.C.T.-C., and J.H. edited and revised manuscript; M.J.A.M.v.P., M.C.T.-C., and J.H. approved final version of manuscript.

REFERENCES

Aladjalova NA. Infra-slow rhythmic oscillations of the steady potential of the cerebral cortex. *Nature* 179: 957–959, 1957.

Aladjalova NA. *Slow Electrical Processes in the Brain*. Amsterdam: Elsevier, 1964.

Albrecht D, Gabriel S. Very slow oscillations of activity in geniculate neurones of urethane-anaesthetized rats. *Neuroreport* 5: 1909–1912, 1994.

Albrecht D, Royl R, Kaneoke Y. Very slow oscillatory activities in lateral geniculate neurons of freely moving and anesthetized rats. *Neurosci Res* 32: 209–220, 1998.

Amzica F, Steriade M. Neuronal and glial membrane potentials during sleep and paroxysmal oscillations in the neocortex. *J Neurosci* 20: 6648–6665, 2000.

Castro-Alamancos MA, Connors BW. Thalamocortical synapses. *Prog Neurobiol* 51: 581–606, 1997.

Cloostermans MC, van Meulen FB, Eertman CJ, Hom HW, van Putten MJAM. Continuous electroencephalography monitoring for early prediction of neurological outcome in postanoxic patients after cardiac arrest: a prospective cohort study. *Crit Care Med* 40: 2867–2875, 2012.

FitzGibbon T, Hayward JS, Walker D. EEG and visual evoked potentials of conscious man during moderate hypothermia. *Electroencephalogr Clin Neurophysiol* 58: 48–54, 1984.

Fox MD, Raichle ME. Spontaneous fluctuations in brain activity observed with functional magnetic resonance imaging. *Nat Rev Neurosci* 8: 700–711, 2007.

He BJ, Snyder AZ, Zempel JM, Smyth MD, Raichle ME. Electrophysiological correlates of the brain's intrinsic large-scale functional architecture. *Proc Natl Acad Sci USA* 105: 16039–16044, 2008.

He J. Slow oscillation in non-lemniscal auditory thalamus. *J Neurosci* 23: 8281–8290, 2003.

Helps S, James C, Debener S, Karl A, Sonuga-Barke EJS. Very low frequency EEG oscillations and the resting brain in young adults: a preliminary study of localisation, stability and association with symptoms of inattention. *J Neural Transm* 115: 279–285, 2008.

Hiltunen T, Kantola J, Abou Elseoud A, Lepola P, Suominen S, Starck T, Nikkinen J, Remes J, Tervonen O, Palva Kiviniemi V, Matias Palva J. Infra-slow EEG fluctuations are correlated with resting-state network dynamics in fMRI. *J Neurosci* 34: 356–362, 2014.

Hindriks R, van Putten MJAM. Meanfield modeling of propofol-induced changes in spontaneous EEG rhythms. *Neuroimage* 60: 2323–2334, 2012.

Hofmeijer J, van Putten MJAM. Ischemic cerebral damage: an appraisal of synaptic failure. *Stroke* 43: 607–615, 2012.

Hofmeijer J, Mulder ATB, Farinha AC, van Putten MJAM, le Feber J. Mild hypoxia affects synaptic connectivity in cultured neuronal networks. *Brain Res* 1557: 180–189, 2014a.

Hofmeijer J, Tjepkema-Cloostermans MC, van Putten MJAM. Burst-suppression with identical bursts: a distinct EEG pattern with poor outcome in postanoxic coma. *Clin Neurophysiol* 125: 947–954, 2014b.

Hughes JR. Extreme stereotypy in the burst suppression pattern. *Clin Electroencephalogr* 17: 162–168, 1986.

Hughes SW, Lorincz MR, Parri HR, Crunelli V. Infraslow ($<$ 0.1 Hz) oscillations in thalamic relay nuclei basic mechanisms and significance to health and disease states. *Prog Brain Res* 193: 145–162, 2011.

Izhikevich EM. *Dynamical Systems in Neuroscience*. MIT Press, Cambridge MA, 2007.

Kemp B, van Beelen T, Stijl M, van Someren P, Roessen M, van Dijk JG. A DC attenuator allows common EEG equipment to record fullband EEG, and fits fullband EEG into standard European data format. *Clin Neurophysiol* 121: 1992–1997, 2010.

Ko AL, Darvas F, Poliakov A, Ojemann J, Sorensen LB. Quasi-periodic fluctuations in default mode network electrophysiology. *J Neurosci* 31: 11728–11732, 2011.

Kochs E. Electrophysiological monitoring and mild hypothermia. *J Neurosurg Anesthesiol* 7: 222–228, 1995.

Kusters AH, Vijn PC, van den Brom WE, Haberham ZL, Venker-van Haagen AJ, Hellebrekers LJ. EEG-burst-suppression-controlled propofol anesthesia in the dog. *Vet Q* 20, *Suppl* 1: S105–S106, 1998.

Liley DTL, Walsh M. The mesoscopic modeling of burst suppression during anesthesia. *Front Comput Neurosci* 7: 1–12, 2013.

Lörincz ML, Geall F, Bao Y, Crunelli V, Hughes SW. ATP-dependent infra-slow ($<$ 0.1 Hz) oscillations in thalamic networks. *PLoS One* 4: e4447, 2009.

Monto S, Palva S, Voipio J, Palva JM. Very slow EEG fluctuations predict the dynamics of stimulus detection and oscillation amplitudes in humans. *J Neurosci* 28: 8268–8272, 2008.

Moujahid A, D'Anjou A, Graca M. Energy demands of diverse spiking cells from the neocortex, hippocampus, and thalamus. *Front Comp Neurosci* 8: 1–12, 2014.

Murphy TH, Li P, Betts K, Liu R. Two-photon imaging of stroke onset in vivo reveals that NMDA-receptor independent ischemic depolarization is the major cause of rapid reversible damage to dendrites and spines. *J Neurosci* 28: 1756–1772, 2008.

Pan WJ, Thompson GJ, Magnuson ME, Jaeger D, Keilholz S. Infraslow LFP correlates to resting-state fMRI BOLD signals. *NeuroImage* 74: 288–297, 2013.

Parri HR, Crunelli V. Pacemaker calcium oscillations in thalamic astrocytes in situ. *Neuroreport* 12: 3897–3900, 2001.

Parri HR, Gould TM, Crunelli V. Spontaneous astrocytic Ca^{2+} oscillations in situ drive NMDAR-mediated neuronal excitation. *Nature Neurosci* 4: 803–812, 2001.

Picchioni DSGH, Fukunaga BM, Carr WS, Meltzer J, Balkin TJ, Duyn JH, Braun AR. NIH Public Access. *Brain Res* 1374: 63–72, 2012.

Picchioni DSGH, Horovitz SG, Fukunaga M, Carr WS, Meltzer JA, Balkin TJ, Duyn JH, Braun AR. Infraslow EEG oscillations organize large-scale cortical-subcortical interactions during sleep: a combined EEG/fMRI study. *Brain Res* 1374: 63–72, 2011.

R Development Core Team. *R: A Language and Environment for Statistical Computing*. R Foundation for Statistical Computing, Vienna, Austria: 2008.

Raichle ME, MacLeod AM, Snyder AZ, Powers WJ, Gusnard DA, Shulman GL. A default mode of brain function. *Proc Natl Acad Sci USA* 98: 676–682, 2001.

Reddy RV, Moorthy SS, Mattice T, Dierdorf SF, Deitch RD Jr. An electroencephalographic comparison of effects of propofol and methohexital. *Electroencephalogr Clin Neurophysiol* 83: 162–168, 1992.

Rodin E, Constantino T, Bigelow J. Interictal infraslow activity in patients with epilepsy. *Clin Neurophysiol* 125: 919–929, 2014.

Rosazza C, Minati L. Resting-state brain networks: literature review and clinical applications. *Neurol Sci* 32: 773–785, 2011.

Rossetti AO, Oddo M, Logroscino G, Kaplan PW. Prognostication after cardiac arrest and hypothermia. A prospective study. *Ann Neurol* 67: 301–307, 2010.

Schroeder CE, Lakatos P. Low-frequency neuronal oscillations as instruments of sensory selection. *Trends Neurosci* 32: 1–16, 2009.

Steriade M, Amzica F, Contreras D. Cortical and thalamic cellular correlates of electroencephalographic burst-suppression. *Electroencephalogr Clin Neurophysiol* 90: 1–16, 1994.

Tabak J, Senn W, O'Donovan MJ, Rinzel J. Modeling of spontaneous activity in developing spinal cord using activity-dependent depression in an excitatory network. *J Neurosci* 20: 3041–3056, 2000.

Tjepkema-Cloostermans MC, Hofmeijer J, Trof RJ, Blans MJ, Beishuizen A, van Putten MJAM. Electroencephalogram predicts outcome in patients with postanoxic coma during mild therapeutic hypothermia. *Crit Care Med* 43: 159–167, 2015.

Tort ABL, Komorowski R, Eichenbaum H, Kopell N. Measuring phase-amplitude coupling between neuronal oscillations of different frequencies. *J Neurophysiol* 104: 1195–1210, 2010.

van Putten MJAM. The N20 in post-anoxic coma: are you listening? *Clin Neurophysiol* 123: 1460–1464, 2012.

van Putten MJAM, van Putten MHPM. Uncommon EEG burst-suppression in severe postanoxic encephalopathy. *Clin Neurophysiol* 121: 1213–1219, 2010.

Vanhatalo S, Palva JM, Holmes MD, Miller JW, Voipio J, Kaila K. Infraslow oscillations modulate excitability and interictal epileptic activity in the human cortex during sleep. *Proc Natl Acad Sci USA* 101: 5053–5057, 2004.

Vanhatalo S, Voipio J, Kaila K. Full-band EEG (FbEEG): an emerging standard in electroencephalography. *Clin Neurophysiol* 116: 1–8, 2005.

Voipio J, Tallgren P, Heinonen E, Vanhatalo S, Kaila K. Millivolt-scale DC shifts in the human scalp EEG: evidence for a nonneuronal generator. *J Neurophysiol* 89: 2208–2214, 2003.

Whitten TA, Martz LJ, Guico A, Gervais N, Dickson CT. Heat synch: inter- and independence of body-temperature fluctuations and brain-state alternations in urethane-anesthetized rats. *J Neurophysiol* 102: 1647–1656, 2009.

Wu D, Xiong W, Jia X, Geocadin RG, Thakor NV. Short- and long-latency somatosensory neuronal responses reveal selective brain injury and effect of hypothermia in global hypoxic ischemia. *J Neurophysiol* 107: 1164–1171, 2012.

Zanatta P, Toffolo GM, Sartori E, Bet A, Baldanzi F, Agarwal N, Golanov E. The human brain pacemaker: Synchronized infra-slow neurovascular coupling in patients undergoing non-pulsatile cardiopulmonary bypass. *Neuroimage* 72: 10–19, 2013.

Zelmann R, Lina JM, Schulze-Bonhage A, Gotman J, Jacobs J. Scalp EEG is not a blur: it can see high frequency oscillations although their generators are small. *Brain Topogr* 27: 683–704, 2014.